Electronic Supplementary Information for

Phase segregated $Cu_{2-x}Se/Ni_3Se_4$ bimetallic selenide nanocrystals formed through cation exchange reaction for active water oxidation precatalyst

Sungwon Kim,[a] Hiroki Mizuno,[a] Masaki Saruyama,[b] Masanori Sakamoto,[b] Mitsutaka Haruta,[a] Hiroki Kurata,[a] Taro Yamada,[c] Kazunari Domen[c] and Toshiharu Teranishi*[b]

[a]Department of Chemistry, Graduate School of Science, Kyoto University, Gokasho, Uji, Kyoto 611-0011, Japan.

[b]Institute for Chemical Research, Kyoto University, Gokasho, Uji, Kyoto 611-0011, Japan.

[c]Department of Chemical System Engineering, The University of Tokyo, 7-3-1, Hongo, Bunkyo-ku, Tokyo 113-8656, Japan.

Email: teranisi@scl.kyoto-u.ac.jp

Experimental details

Chemicals: Nickel (II) acetylacetonate (Ni(acac)$_2$, 95%), selenium (Se, 99.99%), 1-octadecene (ODE, 90%), oleic acid (OLAc, 90%), and tri-n-octylphosphine (TOP, 97%) were purchased from Sigma-Aldrich. Oleylamine (OLAm, 80–90%) was purchased from Acros-Organics. Copper (I) chloride (CuCl, 95%) and nickel (II) acetate tetrahydrate ($Ni(OAc)_2·4H_2O$, 99.9%) were purchased from Wako Pure Chemical Industries. All chemicals were used without further purification.

Synthesis of ber-$Cu_{2-x}Se$ NCs: An OLAm solution of Se (stock solution) was prepared by dissolving Se (2 mmol) in ODE (20 mL) at 220 °C for 3 h under N_2 atmosphere. During this process, the colour changed from black to red and finally turned clear yellow. In a separate flask, the above stock solution was injected into the mixture of CuCl (2 mmol), OLAm (12 mmol), and OLAc (4 mmol). The flask was de-gassed under vacuum at 100 °C for 1 h and then heated to 220 °C un-der an N2 blanket. The solution was maintained at 220 °C for 1 h and subsequently cooled down to room temperature. The NCs were precipitated by acetone, followed by centrifugation and decantation. The collected NCs were washed with hexane and acetone.

Cation exchange reaction between ber-$Cu_{2-x}Se$ NCs and Ni pre-cursors: In a cation exchange reaction of the ber-$Cu_{2-x}Se$ NCs with Ni^{2+} ions, Ni(acac)$_2$ or $Ni(OAc)_2·4H_2O$ (4 mmol) in OLAm (8 mL) and ODE (16 mL) was degassed under vacuum in a flask at 100 °C for 1 h. Then the flask was filled with N_2 and the temperature was raised to 140 °C. At this point the ber-$Cu_{2-x}Se$ NCs (2 mmol) dispersed in ODE (4 mL) by sonication and TOP (8 mL) were subsequently added to the above flask. After the mixture was stirred at 140 °C, the resulting NCs were cooled and precipitated by ethanol, followed by centrifugation and decantation. The collected NCs were further washed with a mixture of hexane and ethanol. After the purification step, a small amount of OLAm (10 µL) was added to stabilize the NCs dispersed in hexane solution.

Cation exchange reaction of ber-$Cu_{2-x}Se$ NCs without Ni precursors: For the characterization of the partial etching process during the cation exchange reaction, a control experiment was carried out in the absence of Ni precursors. The synthetic procedure was the same as the typical cation exchange reaction except for the absence of Ni precursor. The reaction was terminated at 10 min after the TOP injection.

Structural and elemental analysis: TEM observation was performed on a JEM1011 (JEOL) operated at 100 kV. HRTEM and STEM-EDS measurements were performed on a JEM-ARM200F (JEOL) operated at 200 kV. SEM observation was performed on an S-4800 (Hitachi). XRD measurement was conducted on a PANalytical X'Pert Pro MPD with CuKα radiation (λ = 1.542 Å) operated at 45 kV and 40 mA. XPS measurement was conducted in an ultrahigh vacuum combined system equipped with a hemispherical electron analyser (Omicron model EA125) and a twin-anode (Mg/Al) X-ray source (Vacuum Generators). UV-Vis-NIR absorption spectra were measured on a U-3310 spectrophotometer (Hitachi). XRF measurement was performed on an Element Analyser JSX-3202X (JEOL).

Preparation of NCs-loaded carbon paper electrodes: A 1 × 2 cm^2 piece of carbon paper (MGL370) was washed with hexane, ethanol, and acetone. The cleaned carbon paper was dried under vacuum. A hexane solution of 0.5 mg cm^{-2} of ber-$Cu_{2-x}Se$, ber-$Cu_{2-x}Se$/sp-Ni_3Se_4, or sp-Ni_3Se_4 NCs was dropped onto the carbon paper and dried under vacuum. No treatment was conducted for removing ligands. The NCs-deposited area was 0.5–0.8 cm^2.

Electrochemical measurements: Electrochemical measurements were performed at room temperature using a three-electrode system with an ALS620C electrochemical analyser (BAS). Ag/AgCl (3 M NaCl) was used as a reference electrode in 0.1 M KOH (pH 13) electrolyte. Pt wire was used as a counter electrode. Before the measurements, the electrolyte was degassed by bubbling with Ar gas for 30 min. During the measurements, the electrolyte solution was stirred. All the voltammograms were *iR*-corrected to account for uncompensated solution resistance (*R*). The *R* value was measured with an accessory of the analyser based on a previously reported technique (P. He and L. R. Faulkner, *Anal. Chem.*, 1986, **58**, 517-523.). The measured potentials vs Ag/AgCl were converted to those vs the reversible hydro-gen electrode (RHE) scale using the Nernst equation. Before comparing the activities, 50 cycles scanning were applied for the activation of NCs (Fig. S20). Electrochemical impedance spectroscopy (EIS) tests were carried out at overpotential of 0.35 V applying 5 mV AC voltage in the frequency range from 10^6 Hz to 10^{-1} Hz.

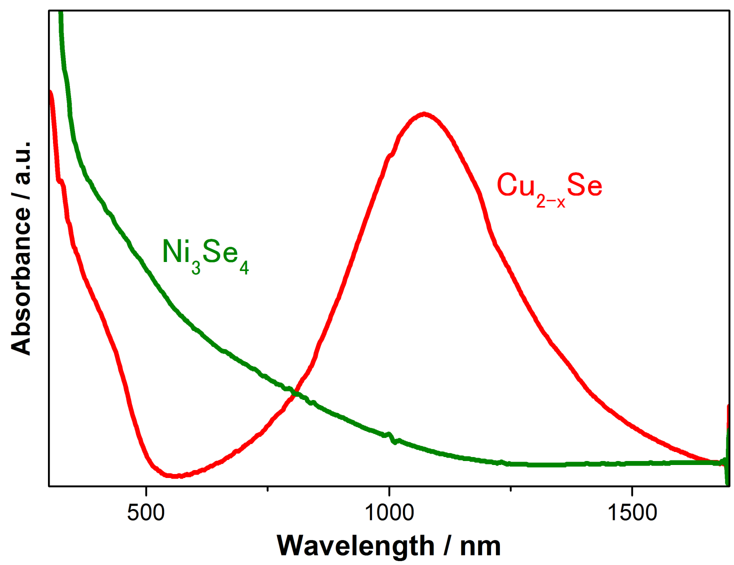

Fig. S1 UV-Vis-NIR spectra of ber-$Cu_{2-x}Se$ NCs (red line) and sp-Ni_3Se_4 NCs after 15 min in cation exchange reaction (green line).

Table S1 Evolution of composition (by XRF) of ber-$Cu_{2-x}Se$ NCs during the cation exchange reaction using $Ni(OAc)_2$ as Ni precursor.

Reaction time / min	Composition / mol%		
	Cu	Ni	Se
0	64	0	36
15	0	56	44
30	0	59	41
45	0	58	42
60	0	59	41

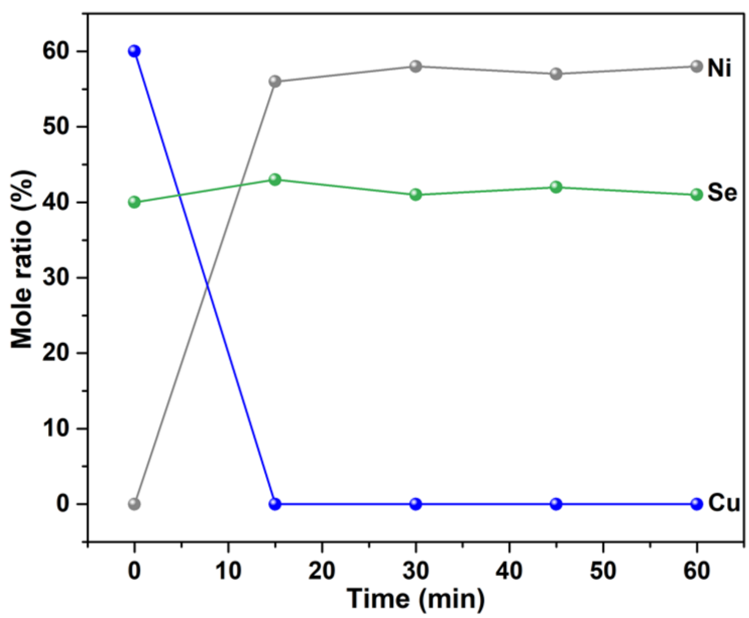

Fig. S2 Change in molar ratios of elements in ber-$Cu_{2-x}Se$ NCs at various cation exchange reaction times using $Ni(OAc)_2$ as Ni precursor according to Table S1.

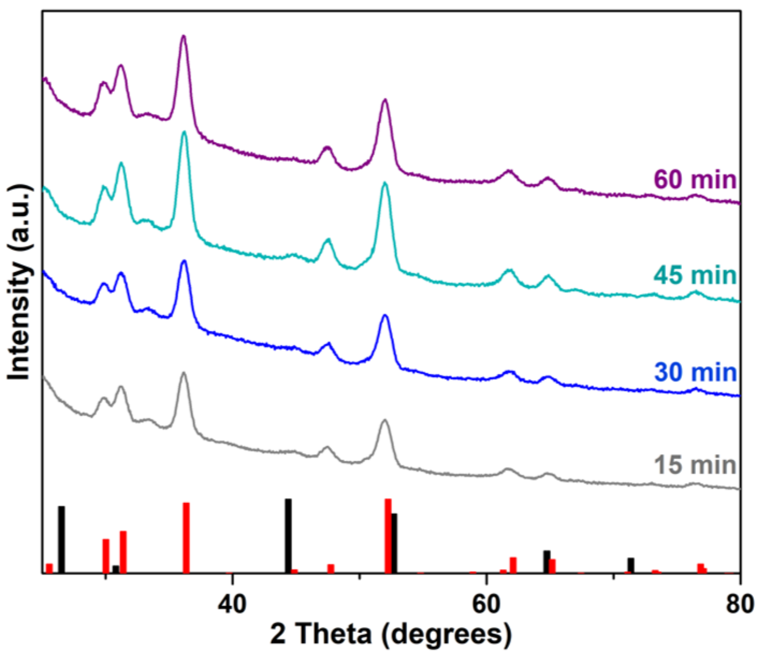

Fig. S3 XRD patterns of the products during the cation exchange reaction from ber-$Cu_{2-x}Se$ NCs to sp-Ni_3Se_4 NCs using $Ni(OAc)_2$. The reference peaks of sp-Ni_3Se_4 (red) and ber-$Cu_{2-x}Se$ (black) phases are also shown in the bottom.

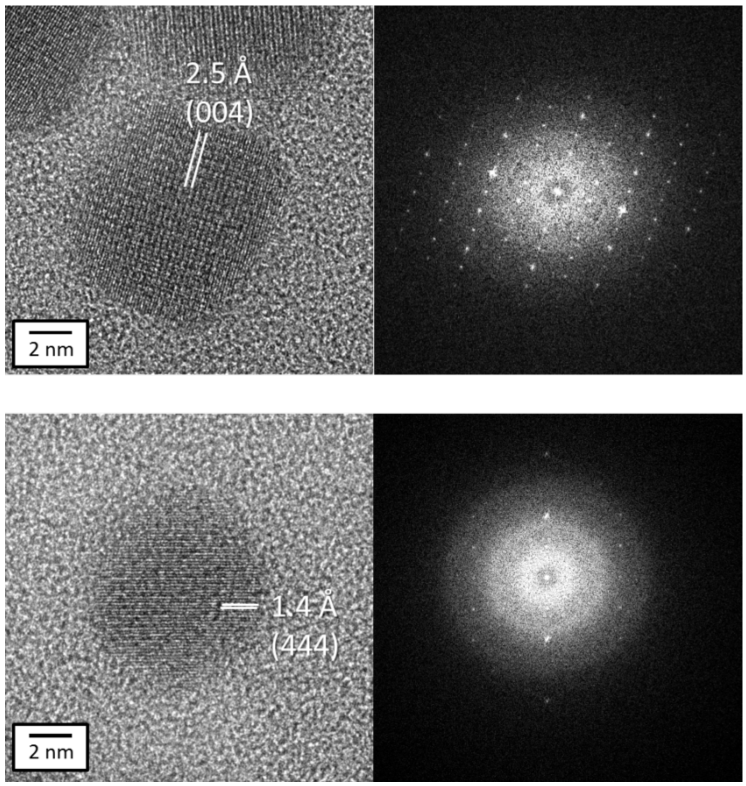

Fig. S4 Additional HRTEM images of sp-Ni_3Se_4 NCs and their FFT patterns.

Table S2 The crystal structure information of the spinel Ni_3Se_4.

Structure parameters:

Crystal system: Cubic

Space group: Fd-3m

a = 9.94 Å

Unit cell volume = 982.10 $Å^3$

	x	y	z	occ.
Se	0.2444	0.2444	0.2444	1.00
Ni1	0.3750	0.3750	0.3750	1.00
Ni2	0.0000	0.0000	0.0000	1.00

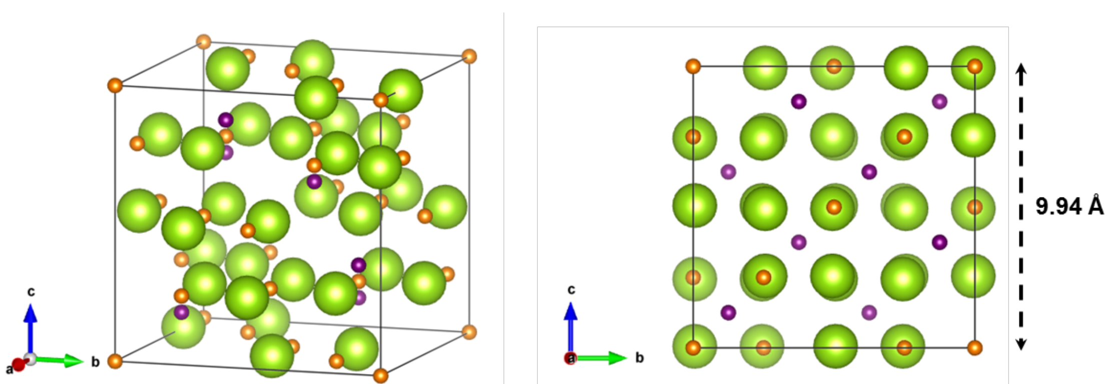

Fig. S5 Unit cells of sp-Ni_3Se_4. Tetrahedral Ni1 and Octahedral Ni2 are colored in purple and orange, respectively.

Table S3 Comparison of crystal structure, morphology and synthetic procedure of artificial Ni selenide system in the literature.

Crystal structure	Morphology	Producer	Refence
Cubic $NiSe_2$	Particulate film	Elecrodeposition	[1]
Hexagonal NiSe	~µm pillar	Solvothermal selenization	[2]
Cubic $NiSe_2$	~µm plate	Selenization of MOF	[3]
Rhombohedral Ni_3Se_2 Hexagonal NiSe	Particulate spheres	Hydrothermal	[4]
Rhombohedral Ni_3Se_2	~µm flower-shape	Electrochemical deposition	[5]
Cubic $NiSe_2$	Nanosheet	Hydrothermal	[6]
Cubic $NiSe_2$ Hexagonal NiSe Rhombohedral Ni_3Se_2	Microsphere	Hydrothermal	[7]
Rhombohedral Ni_3Se_2	Nanoforest	Hydrothermal	[8]
Hexagonal NiSe	~µm wire/sphere/hexagon	Hydrothermal	[9]
Mixed-Cubic-Orthorombic $NiSe_2$	Nanosphere	Electrospinning/selenization	[10]
Cubic $NiSe_2$	Particulate film	Electrodeposition	[11]
Monoclinic Ni_3Se_4	Hierarchical array	Microwave	[12]
Monoclinic Ni_3Se_4	Nanorod array	Hydrothermal	[13]

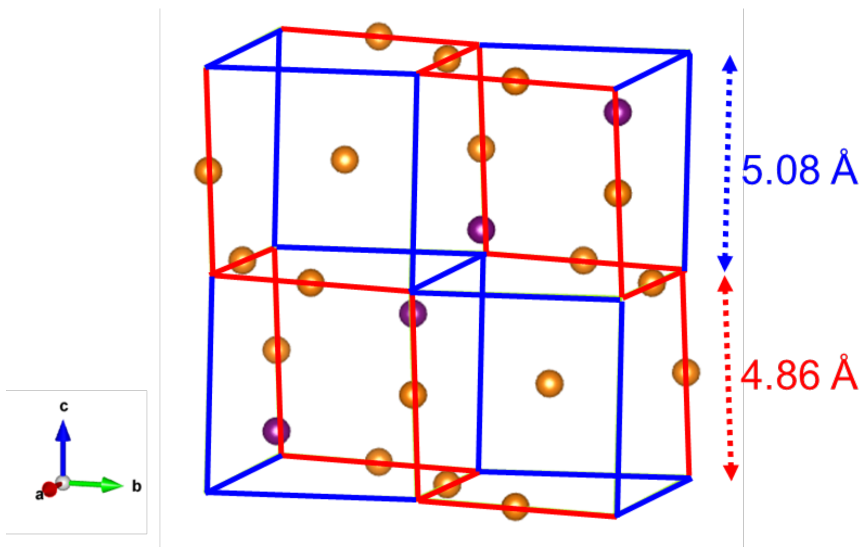

Fig. S6 Wireframe depiction of (1x2x2) Unit cells of Se sub-lattice of sp-Ni_3Se_4. Blue and red lines show 5.08 Å and 4.86 Å sides, respectively, which emphasize the lattice distortion of Se sub-lattice. Tetrahedral Ni1 and Octahedral Ni2 are colored in purple and orange, respectively.

Table S4. The number of each cation sites in the lattices in Figure 2a.

Cu sites	number of sites		Ni sites	number of sites
Tetrahedral Cu1	64	→	Tetrahedral Ni1	8
non tetrahedral C2	256	→	empty	0
empty	0	→	Octahedral Ni2	16

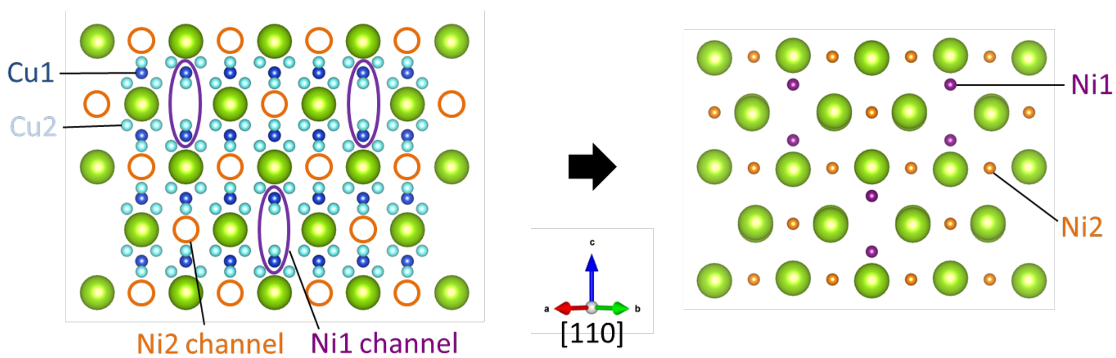

Fig. S7 Parallel images of ber-$Cu_{2-x}Se$ (left, 2×2×2 = 8 unit cells) and sp-Ni_3Se_4 (right, 1 unit cell) along [110] zone axis. Description of channels for Ni1 and Ni2 sites in ber-$Cu_{2-x}Se$ as purple and orange circles, respectively.

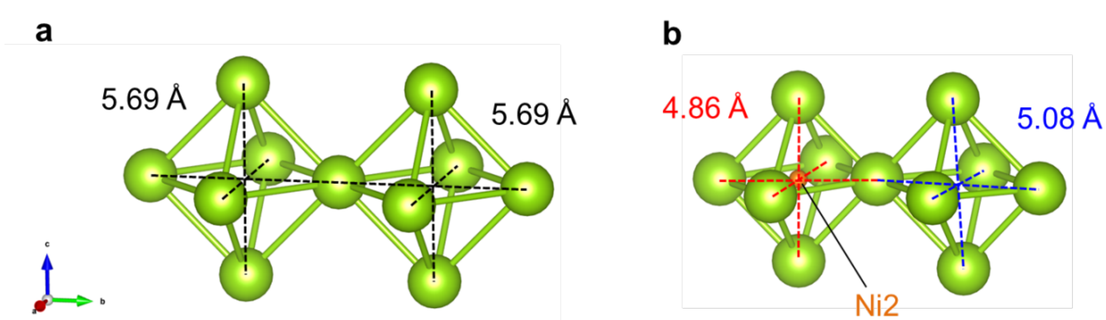

Fig. S8 Neighboring Se octahedra in (a) ber-$Cu_{2-x}Se$ and (b) sp-Ni_3Se_4. Diagonal distances highlight the size of each octahedra. Octahedron with Ni center is smaller than that without Ni.

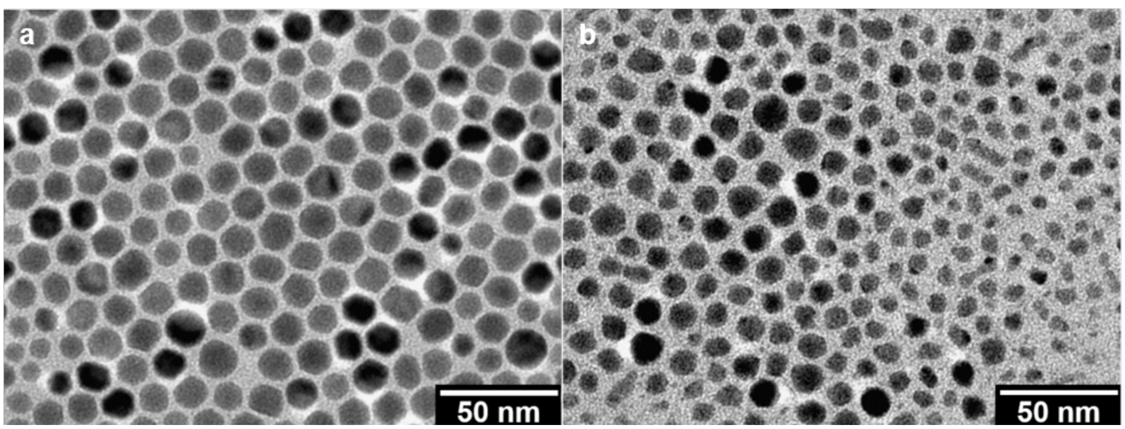

Fig. S9 (a-b) TEM images of (a) as-synthesized ber-$Cu_{2-x}Se$ NCs (16 ± 1.3 nm) and (b) ber-$Cu_{2-x}Se$ NCs after the control cation exchange reaction without Ni precursor (10 ± 1.6 nm).

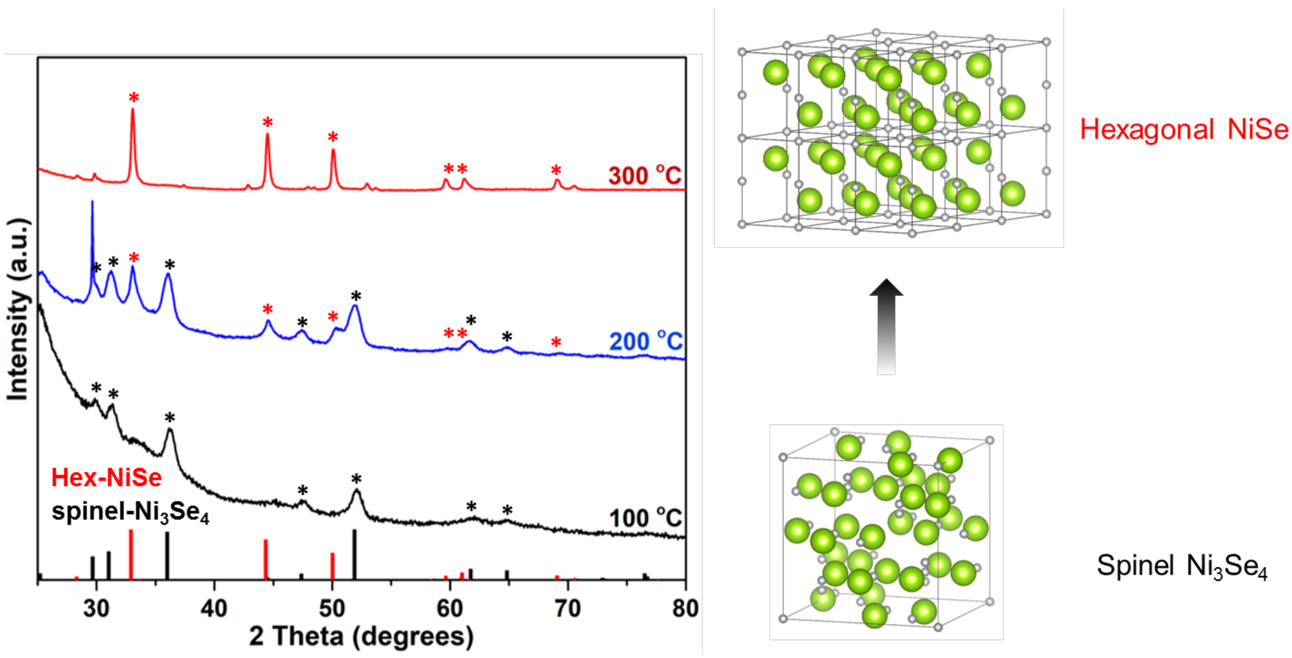

Fig. S10 XRD patterns of the sp-Ni_3Se_4 NCs after annealing under the Ar atmosphere at different temperatures for 1 h. The reference peaks of sp-Ni_3Se_4 (black) and hexagonal NiSe (red) phases are also shown.

Table S5 Composition evolution of the ber-$Cu_{2-x}Se$ NCs during the cation exchange reaction using $Ni(acac)_2$ as Ni precursor determined by XRF.

Reaction time / min	Composition / mol%		
	Cu	Ni	Se
0	64	0	36
15	48	12	40
30	37	21	42
45	26	32	42
60	17	39	44

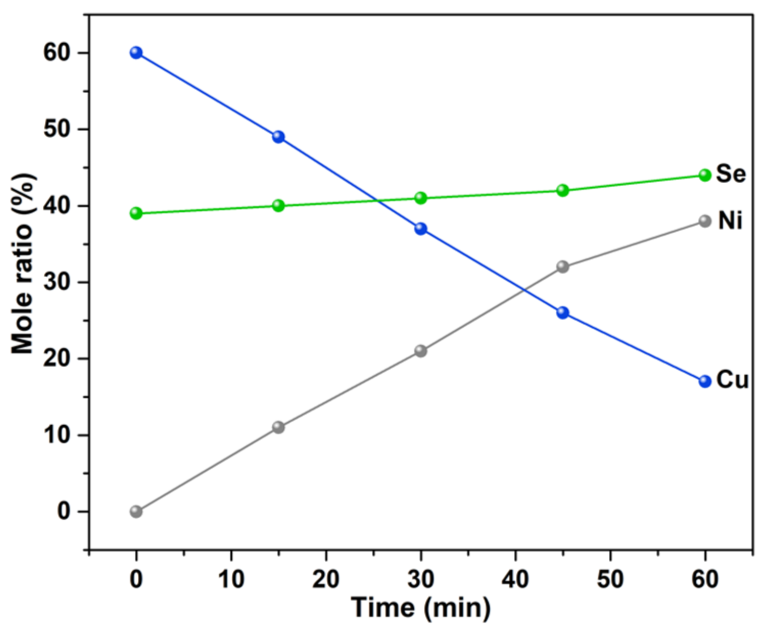

Fig. S11 Change in molar ratio of elements in ber-$Cu_{2-x}Se$ NCs at various cation exchange reaction times using $Ni(acac)_2$ as Ni precursor according to Table S3.

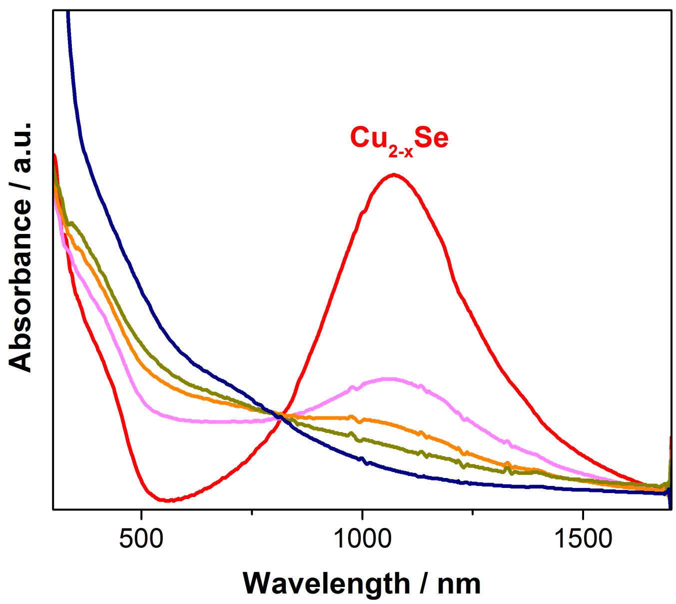

Fig. S12 UV-Vis-NIR spectra of ber-$Cu_{2-x}Se$ NCs (red line) and ber-$Cu_{2-x}Se$/sp-Ni_3Se_4 NCs at different CE reaction time; red: 0 min (ber-$Cu_{2-x}Se$ NCs), pink: 15 min, orange: 30 min, dark yellow: 45 min and navy: 60 min.

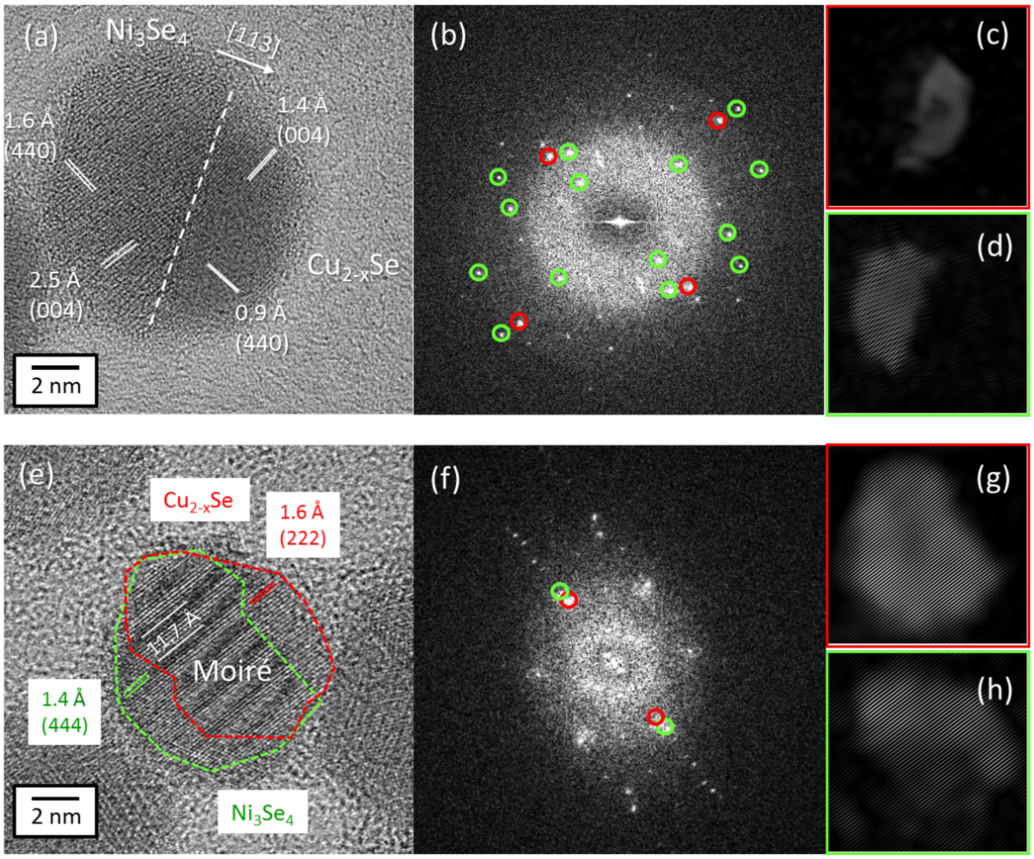

Fig. S13 (a,e) Additional HRTEM images of ber-$Cu_{2-x}Se$/sp-Ni_3Se_4 HNCs and (b,f) their FFT patterns. (c-d and g-h) Inverse FFT images from FFT of b and f, respectively.

Table S6 OER performance comparison of recently reported Ni and Cu based chalcogenide catalysts.

Catalyst	Morphology	Electrolyte	η@10 mA cm^{-2}	Loading amount / mg cm^{-2}	Reference
$Cu_{2-x}Se$-Ni_3Se_4	11 nm NCs	0.1 M KOH	230	0.5	This work
Ni_3Se_4	11 nm NCs	0.1 M KOH	250	0.5	This work
$(Ni, Co)_{0.85}Se$	60 nm nanotube	1 M KOH	255	5	[14]
NiSe/NF	~80 nm nanowire	1 M KOH	270 @ 20 mA cm^{-2}	2.8	[15]
Holey $NiCo_2Se_4$	Nanosheet	1 M KOH	295	1	[16]
$Fe_{0.09}Co_{0.13}$-$NiSe_2$	Porous nanosheet	1 M KOH	251	No data	[17]
$(Ni, Co)Se_2$-GA	~270 nm nanocube	1 M KOH	250	2.8	[18]
Co-Cu_7S_4	60 nm nanodisk	1 M KOH	270	1	[19]

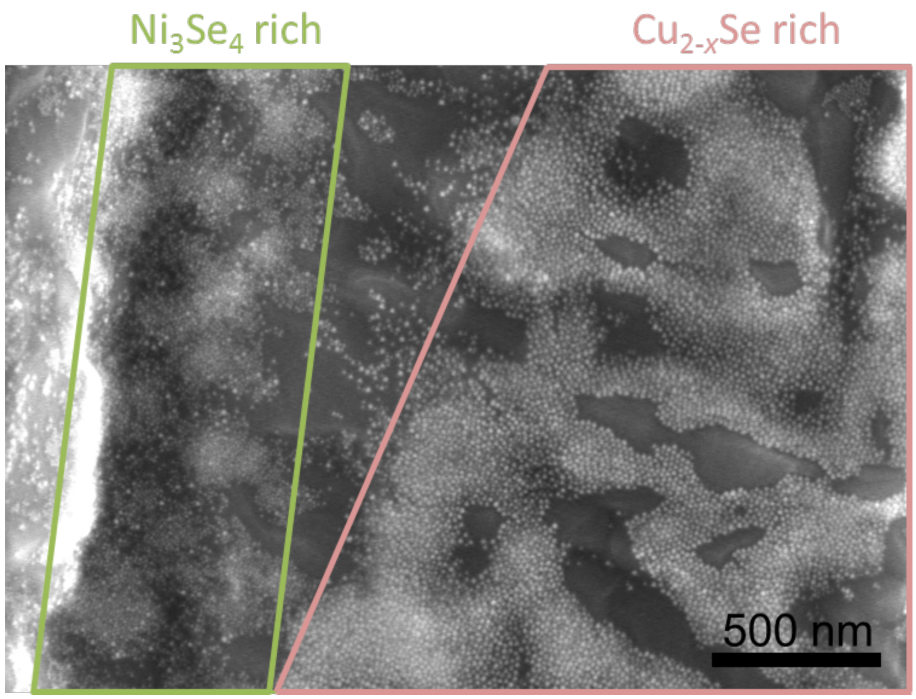

Fig. S14 SEM image of the mixture of ber-$Cu_{2-x}Se$ NCs and sp-Ni_3Se_4 NCs on carbon paper.

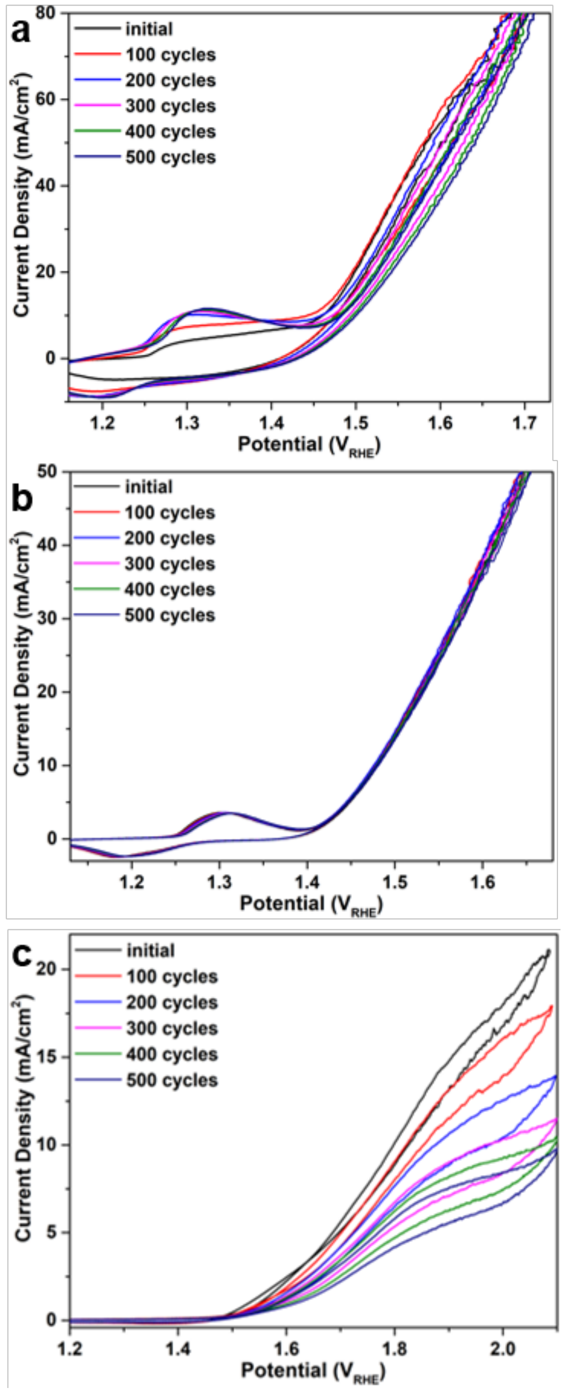

Fig. S15 Cyclic voltammograms of (a) ber-$Cu_{2-x}Se$/sp-Ni_3Se_4 HNCs, (b) sp-Ni_3Se_4 NCs and (c) ber-$Cu_{2-x}Se$ NCs in 0.1 M KOH at initial, 100, 200, 300, 400 and 500 cycled sweeps.

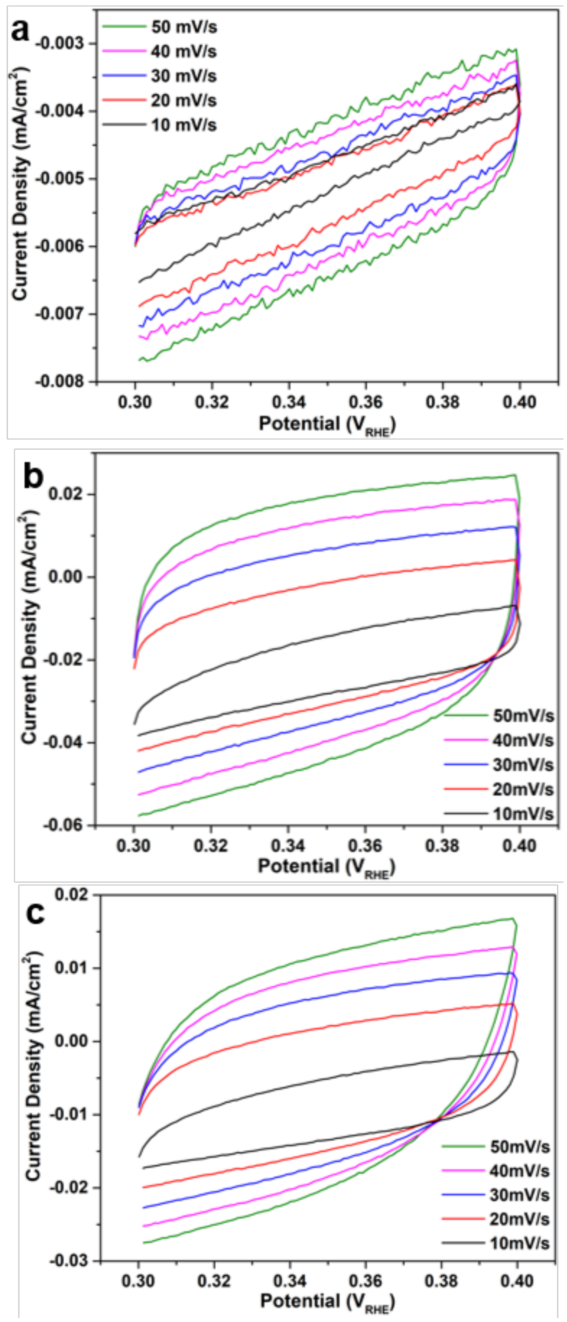

Fig. S16 CV curves of (a) ber-$Cu_{2-x}Se$ NCs, (b) ber-$Cu_{2-x}Se$/sp-Ni_3Se_4 HNCs and (b) sp-Ni_3Se_4 NCs at scan rates of 10 to 50 mV s^{-1} in the range of potential where no Faradaic current does not flow.

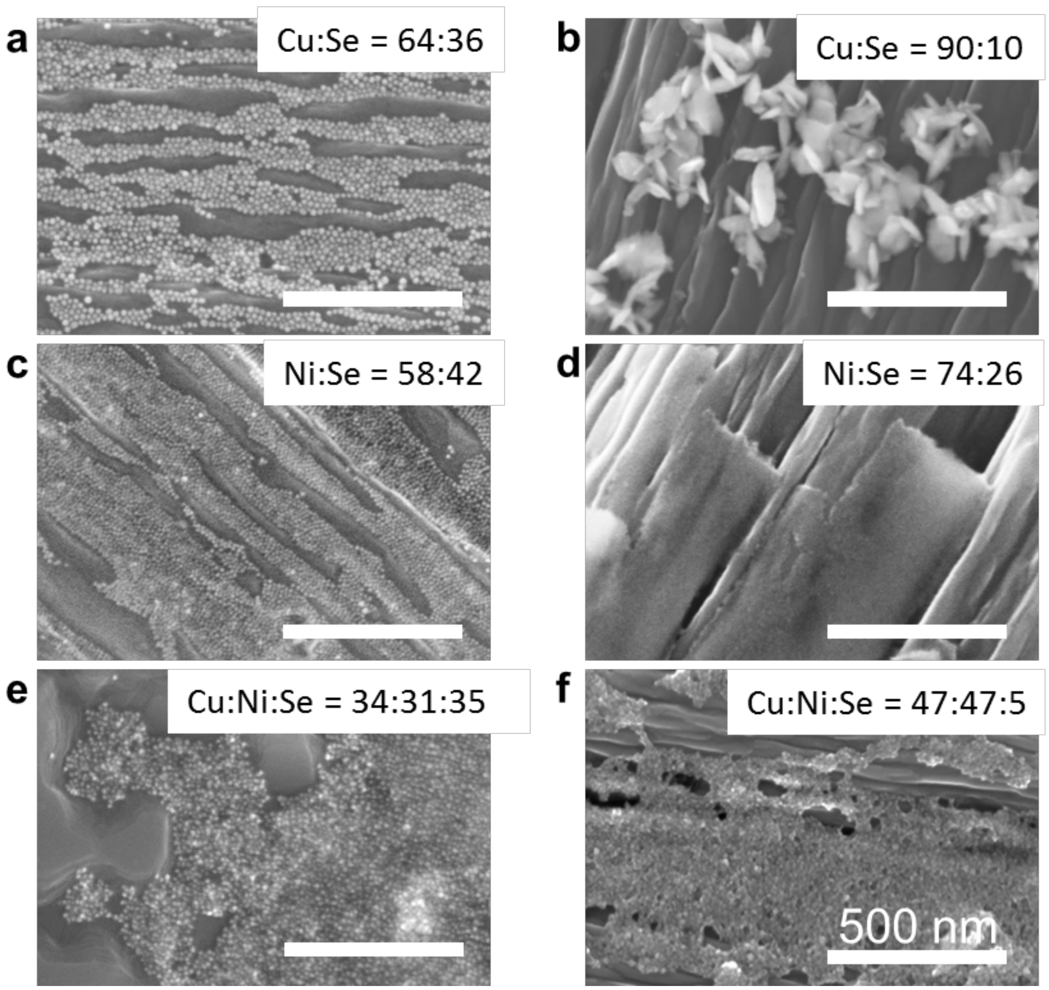

Fig. S17 SEM images of (a,b) ber-$Cu_{2-x}Se$ NCs, (c,d) sp-Ni_3Se_4 NCs and (e,f) ber-$Cu_{2-x}Se$/sp-Ni_3Se_4 HNCs loaded on carbon paper electrodes (a,c,e) before and (b,d,e) after 500 CV sweeps between 1.1 and 1.7 V vs. RHE in 0.1 M KOH.

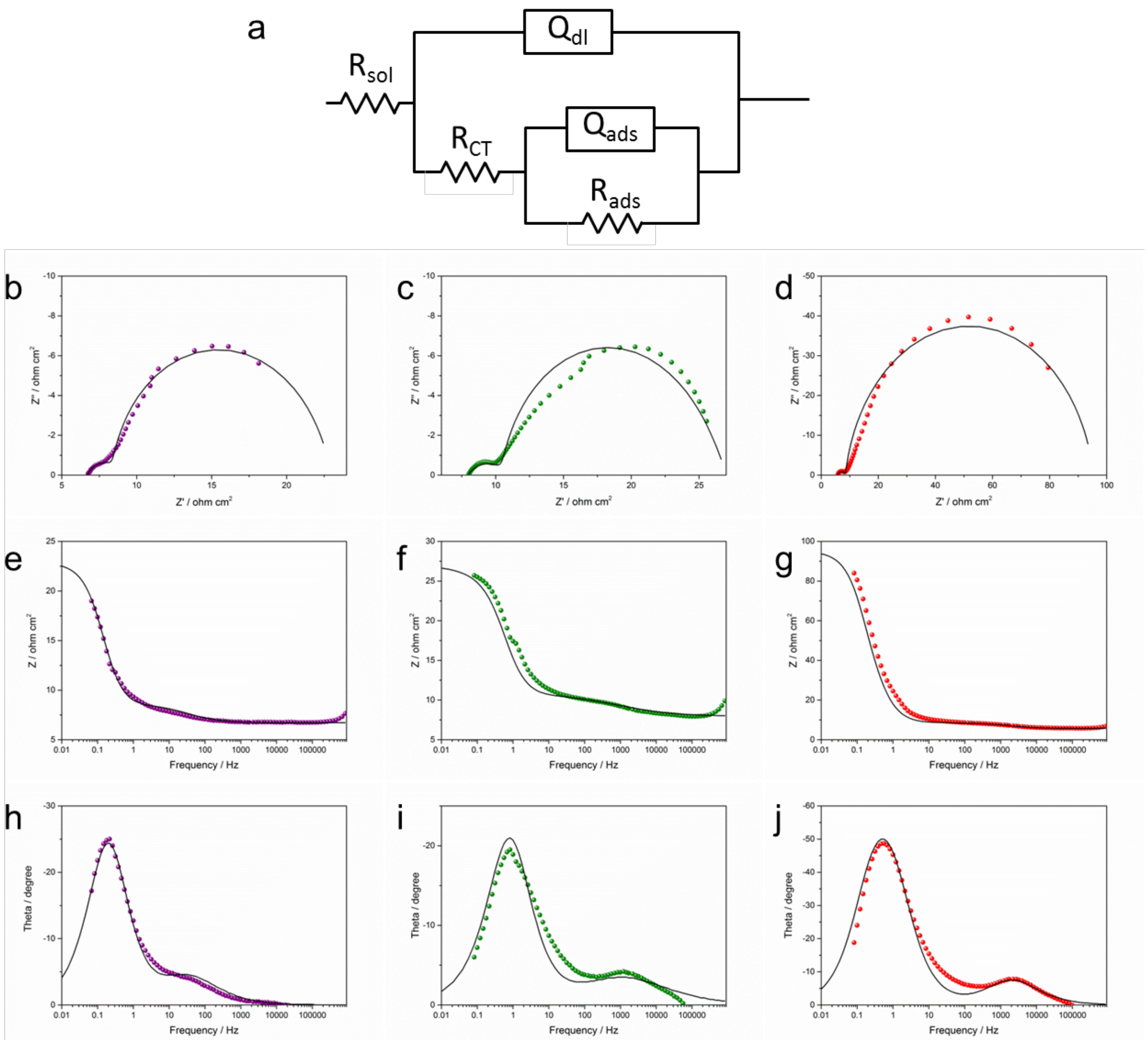

Fig. S18. (a) The equivalent circuit for fitting EIS data. (b-d) Nyquist and (d-i) Bode plots of each NCs. Solid lines are simulated using the equivalent circuit of (a).

Table S7. Fitting parameters for each catalyst.

	R_{sol} / ohm cm^2	R_{CT} / ohm cm^2	Q_{dl} / 10^{-3}ohm^{-1} s^n cm^{-2} (n)	R_{ads} / ohm cm^2	Q_{ads} / 10^{-3}ohm^{-1} s^n cm^{-2} (n)	C_{ads} / 10^{-3}ohm^{-1} s cm^{-2}
$Cu_{2-x}Se$-Ni_3Se_4	6.72	2.04	15 (0.68)	14.2	82 (0.95)	83
Ni_3Se_4	7.96	2.84	5.8 (0.48)	16.3	21 (0.90)	19
$Cu_{2-x}Se$	5.77	2.80	0.36 (0.75)	86.8	13 (0.91)	13

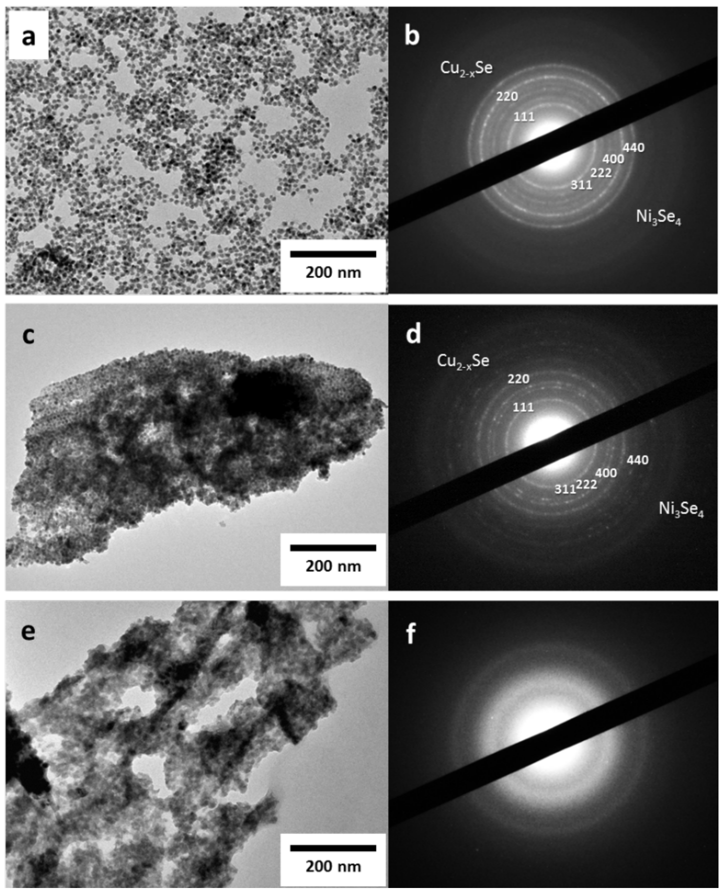

Fig. S19 (a,c,e) TEM images and (b,d,f) SAED patterns of ber-$Cu_{2-x}Se$/sp-Ni_3Se_4 HNCs: (a,b) as-synthesized, (c,d) immersed in 0.1 M KOH electrolyte and (e,f) after 500 cycles CV.

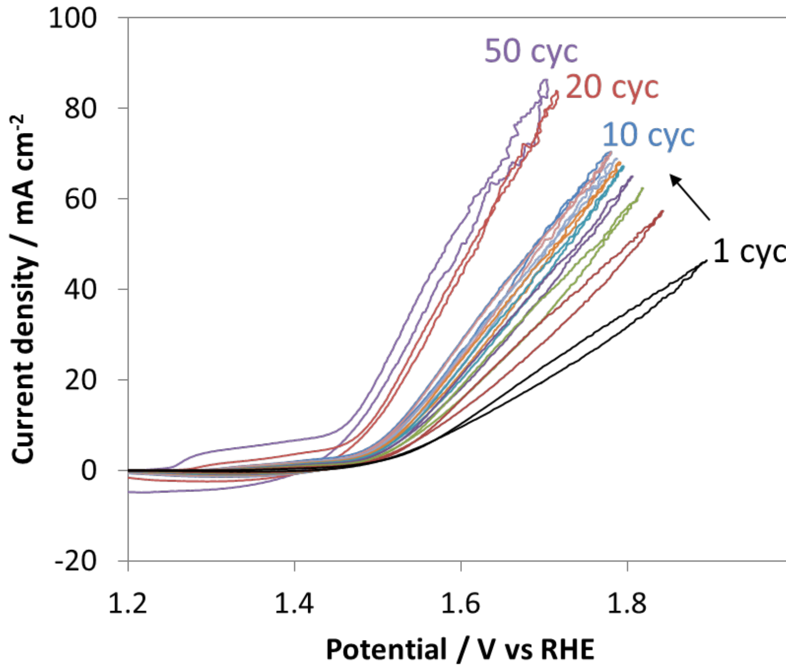

Fig. S20 CVs of ber-$Cu_{2-x}Se$/sp-Ni_3Se_4 HNCs from 1st to 50th cycles.

References

1 Z. Pu, Y. Luo, A. M. Asiri and X. Sun, *ACS Appl. Mater. Interfaces*, 2016, **8**, 4718-4723.

2 X. Li, G. Han, Y. Liu, B. Dong, W. Hu, X. Shang, Y. Chai and C. Liu, *ACS Appl. Mater. Interfaces*, 2016, **8**, 20057-20066.

3 H. Fan, H. Yu, X. Wu, Z. Yu, Y. Zhang, Z. Luo, H. Wang, Y. Guo, S. Madhavi and Q. Yan, *ACS Appl. Mater. Interfaces*, 2016, **8**, 25261-25267.

4 K. Xu, H. Ding, H. Lv, S. Tao, P. Chen, X. Wu, W. Chu, C. Wu and Y. Xie, *ACS Catal*., 2017, ***7***, 1, 310-315.

5 G. Nagaraju, S. M. Cha, S. C. Sekhar and J. S. Yu, *Adv. Energy Mater*., 2017, **7**, 1601362, 1-13.

6 F. Wang, Y. Li, T. A. Shifa, K. Liu, F. Wang, Z. Wang, P. Xu, Q. Wang and J. He, *Angew. Chem. Int. Ed*., 2016, **55**, 6919-6924.

7 Z. Zhuang, Q. Peng, J. Zhuang, X. Wang and Y. Li, *Chem. Eur. J*., 2006, **12**, 211-217.

8 R. Xu, R. Wu, Y. Shi, J. Zhang and B. Zhang, *Nano Energy*, 2016, **24**, 103-110.

9 S. Kukunuri, M. R. Krishnan and S. Sampath, *Phys. Chem. Chem. Phys*., 2015, **17**, 23448-23459.

10 J. S. Cho, S. Y. Lee and Y. C. Kang, *Sci. Rep*., 2016, **6**, 23338, 1-10.

11 A. T. Swesi, J. Masud, W. P. R. Liyanage, S. Umapathi, E. Bohannan, J. Medvedeva and M. Nath, *Sci. Rep*., 2017, **7**, 2401, 1-11.

12 S. Ananthara, J. Kennedy and S. Kundu, *ACS Appl. Mater. Interfaces*, 2017, **9**, 8714-8728.

13 J. Y. Zhang, X. Tian, T. He, S. Zaman, M. Miao, Y. Yan, K. Qi, Z. Dong, H. Liu and B. Y. Xia, *J. Mater. Chem. A*, 2018, **6**, 15653-15658.

14 C. Xia, Q. Jiang, C. Zhao, M. N. Hedhili and H. N. Alshareef, *Adv. Mater.*, 2016, **28**, 77-85.

15 C. Tang, N. Cheng, Z. Pu, W. Xing and X. Sun, *Angew. Chem*., 2015, **127**, 9483-9487.

16 Z. Fang, L. Peng, H. Lv, Y. Zhu, C. Yan, S. Wang, P. Kalyani, X. Wu and G. Yu, *ACS Nano*, 2017, **11**, 9550-9557.

17 Y. Sun, K. Xu, Z. Wei, H. Li, T. Zhang, X. Li, W. Cai, J. Ma, H. J. Fan and Y. Li, *Adv. Mater*., 2018, **30**, 1802121, 1-7.

18 X. Xu, H. Liang, F. Ming, Z. Qi, Y. Xie and Z. Wang, *ACS Catal*., 2017, ***7***, 6394-6399.

19 Q. Li, X. Wang, K. Tang, M. Wang, C. Wang and C. Yan, *ACS Nano*, 2017, **11**, 12230-12239.